

Heme Centers of *Rhodothermus marinus* Respiratory Chain. Characterization of Its *cbb*₃ Oxidase¹

Manuela M. Pereira,² João N. Carita,² Robert Anglin,² Matti Saraste,³ and Miguel Teixeira^{2,4}

Received December 5, 1999; accepted January 16, 2000

Rhodothermus (R.) marinus, a thermohalophilic Gram-negative, and strict aerobic bacterium, has a rather distinct respiratory chain, containing a *caa*₃ terminal oxidase, a novel cytochrome *bc* complex and a HiPIP, which is an electron carrier between this complex and a terminal oxidase (Pereira *et al* (1999a, c). To further elucidate this unusual respiratory system, its membrane-bound heme centers were characterized by visible and EPR spectroscopies as well as by redox potentiometry. *Rhodothermus marinus* contains mostly B- and C-type hemes; a small amount of A-type heme is also detected. The heme centers have relatively low reduction potentials, ranging from ca. +250 to -60 mV, at pH 7. A Rieske-type center was not detected, suggesting the absence of a canonical complex III. The major terminal oxidase expressed by *R. marinus* is a *cbb*₃-type oxidase. Its presence is in agreement with molecular biology studies, which reveal the existence of a gene encoding for a FixN-type oxidase. The oxidase was partially purified and appears to have five subunits, with apparent molecular masses of 64, 57, 36, 26 (C-type heme subunit), and 13 kDa. It contains two low-spin heme C centers, one high-, and one low-spin heme B centers. A full description of the equilibrium redox behavior of the heme centers was obtained for a *cbb*₃ oxidase for the first time. The optical spectrum for each heme center and the corresponding reduction potentials were determined at pH 7: +195 (heme C), +120 (heme B), -50 (heme C), and -50 mV (heme B₃).

KEY WORDS: Terminal oxidase; cytochrome *cbb*₃; thermophile; *Rhodothermus*.

INTRODUCTION

Rhodothermus marinus is a strict aerobic, halophilic marine bacterium, which grows optimally at 65°C and at 1 to 2% sodium chloride. It is a genus related to the group of *Flexibacter*, *Bacteroids*, and *Cytophaga* species (FBC-group) (Andrésson and Frid-

jónsson, 1994). Different *R. marinus* strains were isolated from Iceland (Alfredsson *et al.*, 1988) and from hydrothermal areas on the beach Praia da Ribeira Quente (PRQ) of the island of São Miguel, Azores (strain PRQ) (Nunes *et al.*, 1992), as well as near Naples bay (Moreira *et al.*, 1995). *Rhodothermus marinus* belongs to the small number of known thermophilic aerobic bacteria, which includes *Thermus (T.) thermophilus* ($T_{\text{opt}} = 75^{\circ}\text{C}$), *Bacillus (B.) stearothermophilus*, *Bacillus* PS3 ($T_{\text{opt}} = 65^{\circ}\text{C}$), and *Aquifex pyrofilus* ($T_{\text{opt}} = 95^{\circ}\text{C}$) (Madigan *et al.*, 1997). Because of the subtle balance between the optimal growth temperature and oxygen availability, *R. marinus* thrives under microaerophilic conditions (Kristjansson and Stetter, 1992).

The respiratory chain of *Rhodothermus marinus* has unique characteristics. It was the first bacterium

¹ Key to Abbreviations: TMPD, *N,N,N',N'*-tetramethyl-*p*-phenylenediamine; TMBZ, 3,3',5,5'-tetramethylbenzidine; HiPIP, high-potential iron-sulfur protein; DM, dodecyl β -D-maltoside.

² Instituto de Tecnologia Química e Biológica, Universidade Nova de Lisboa, APT 127, 2780-156, Oeiras, Portugal.

³ European Molecular Biology Laboratory, Meyerhofstrasse 1, W-6900 Heidelberg, Germany.

⁴ Author to whom all correspondence should be sent. email: miguel@itqb.unl.pt.

where a *high-potential iron-sulfur protein* (HiPIP) was found to be membrane bound and proposed to be involved in the respiratory electron transfer chain (Pereira *et al.*, 1994). This HiPIP was recently proved, by an *in vitro* reconstitution experiment, to shuttle electrons between a quinol oxidizing complex and a terminal oxidase, of the *caa₃* type (Pereira *et al.*, 1999a). This role for a HiPIP, as a functional substitute for the canonical *c*-type cytochromes as electron donor to a terminal oxygen reductase, was also proposed to occur in photosynthetic bacteria, through studies with intact membranes (Hochoepler *et al.*, 1995; Bonora *et al.*, 1999). The *caa₃* oxidase also presents unusual characteristics, namely concerning its proton channels: the key glutamate of the D-channel is not present and a tyrosine residue was proposed to be its functional substitute (Pereira *et al.*, 1999b). Very interestingly, *R. marinus* does not appear to contain a *bc₁* complex or its Rieske protein. In its substitution, a novel multiheme complex (cytochrome *bc*) was found, which has menadiol:HiPIP oxidoreductase activity (Pereira *et al.*, 1999c) and may be related to the alternative complex III proposed to be present in *Rhodobacter capsulatus* (Richardson *et al.*, 1989; Bell *et al.*, 1992).

The unusual composition of this electron transfer chain demanded its complete characterization. A detailed study of the spectroscopic and redox behavior of the membrane-bound heme centers of *R. marinus* was undertaken. It was observed that, apart from the cytochrome *bc* complex and the *caa₃* oxidase, as well as a heme-containing succinate dehydrogenase (A. S. Fernandes *et al.*, unpublished data), *R. marinus* expresses a *cbb₃* oxidase as its main terminal oxygen reductase.

MATERIALS AND METHODS

Bacterial Growth

A spontaneous nonpigmented *R. marinus* strain (PRQ 32B) was used in this study. Cell growth was done as in Pereira *et al.* (1999c). Cells were harvested at the mid-exponential, beginning of stationary, and late stationary phases. For protein purification, cells harvested at the last phase were used. The cells were ruptured by passage in a French press and the membrane fraction was obtained as described in Pereira *et al.* (1999c).

Protein Purification

The membrane fraction was successively washed with high- and low-ionic strength buffers, to remove soluble and weakly bound proteins, and solubilized with dodecyl- β -D-maltoside in a ratio of 2 g per gram of protein. All chromatographic steps were done on a Pharmacia HiLoad system at 4°C. The purification steps were monitored by activity measurements (TMPD oxidase) and visible and EPR spectroscopies. The detergent-solubilized extract was applied to a fast-flow DEAE column, equilibrated with 20 mM Tris-HCl, pH 8, 0.1% DM (Buffer A), and eluted in a linear gradient of 0 to 50% 1 M NaCl, in the same buffer. The fraction containing TMPD oxidase activity, which also contains virtually all heme centers, as determined by visible spectroscopy, was then applied to a chelating sepharose fast-flow column saturated with Cu⁺² and equilibrated with buffer A. The fraction containing the *cbb₃* oxidase was eluted in a gradient of 0 to 10% 125 mM imidazole in Buffer A and then applied to a Q-sepharose column. This last column was eluted with a linear gradient of 0 to 50% 1 M NaCl in Buffer A. Applying the fraction containing the *cbb₃* oxidase to other ion exchange, molecular exclusion, HTP or hydrophobic interaction (octyl- and phenyl-Sepharose) columns did not improve the purification of this fraction, as determined by EPR and UV-visible spectra, specific activity, and SDS-PAGE.

Protein and Heme Determination

Protein concentrations were determined using the modified MicroBiuret method for membrane proteins (Watters, 1978). Heme contents were determined by pyridine hemochrome using molar absorptivities of $\epsilon_{r-o,550-535} = 23.97 \text{ mM}^{-1}\text{cm}^{-1}$ for heme C, $\epsilon_{r-o,556-540} = 23.98 \text{ mM}^{-1} \text{ cm}^{-1}$ for heme B, and $\epsilon_{r-o,peak-620} = 25.02 \text{ mM}^{-1} \text{ cm}^{-1}$ for heme A (Berry and Trumpower, 1987). Noncovalently bound hemes were extracted and analyzed as described in Pereira *et al.* (1999b). Standard hemes were obtained from myoglobin and membrane extracts of *E. coli* (B and O hemes), *Acidianus ambivalens* (A_s hemes), and *Paracoccus denitrificans* (A hemes).

Electrophoresis

Tricine-SDS/PAGE was carried out as described by Schägger and von Jagow (1987) with 10%T, 2%C.

The samples were precipitated overnight with acetone and then resuspended in the loading buffer containing 8 M urea. Heme staining was done as in Goodhew *et al.* (1986).

Spectroscopic Techniques

Electronic spectra were obtained on a Beckman DU-70 or on an OLIS DW2 spectrophotometers, at room and liquid nitrogen temperatures. Molar absorptivities of $\epsilon_{592-605} = 3.5 \text{ mM}^{-1}\text{cm}^{-1}$ (cytochrome a_3 , α -band), $\epsilon_{579-558} = 5.5 \text{ mM}^{-1}\text{cm}^{-1}$ (cytochrome b , α -band) (Wood, 1984), and $\epsilon_{429-445} = 91 \text{ mM}^{-1}\text{cm}^{-1}$ (cytochrome a_3 , Soret band) (Anemüller *et al.*, 1994) were used for CO difference spectra. EPR spectra were measured as in Pereira *et al.* (1999c).

Catalytic Activity Assays

TMPD oxidase activity was measured by monitoring the change in absorbance of TMPD at 560 nm at 65°C ($\epsilon_{560} = 12,100 \text{ M}^{-1}\text{cm}^{-1}$). Oxygen consumption was measured polarographically at 35 and at 40°C, with a Clark-type oxygen electrode, YSI Model 5300, Yellow Springs. All assays with solubilized samples were carried out in Buffer A.

Redox Titrations

Anerobic potentiometric titrations, using $\sim 5\text{mV}$ reduction steps, were performed and analyzed as in Pereira *et al.* (1999c). A total of 100 to 150 visible spectra from 400 to 700 nm were recorded for each titration. The data sets were first analyzed by following the absolute and differential absorptions at the Soret and α -bands and, then for the cbb_3 oxidase, the spectra were deconvoluted manually, using the MATLAB software, by visual inspection of each individual spectrum, and by selective subtractions from the total set of redox spectra. Thus, the optical spectrum for each heme center was determined, which allowed the choice of the corresponding maxima at the Soret and α -bands to obtain the individual titration curves. Because of the complexity of the systems, the data were fitted to single Nernst equations, without taking into consideration homotropic (electron–electron) interactions. For the cbb_3 oxidase, the assignment of each optical species was confirmed by selective chemical reductions and

by reaction with carbon monoxide. The relative contributions of each species were deduced from the relative absorbances at each maximum as well as by the area underneath the α -band obtained by weighting, since the transition probabilities are proportional to the spectral area.

DNA Techniques

Genes for terminal oxidases were searched by PCR. For this purpose, a set of mixed oligonucleotide primers was used, corresponding to coding regions of conserved sequences established by alignment of subunit I sequences of cbb_3 terminal oxidases. PCR was performed using Perkin Elmer AmpliTaq DNA polymerase. Assays were done testing different temperatures and MgCl_2 concentrations. General cloning techniques were carried out as described by Ausubel *et al.* (1995). The PCR product, obtained at an annealing temperature of 60°C, was sequenced at EMBL sequencing service and the sequence obtained was compared with protein databases using the NCBI Entrez protein sequence search. Alignments were performed using Clustal W Version 1.6 (Thompson *et al.*, 1997).

RESULTS

Membrane Extract

Rhodothermus marinus cells were cultured under several aeration conditions and harvested at different growth phases. Within experimental error, the membrane extracts obtained show very similar visible and EPR spectra, as well as apparently identical relative heme contents, as judged by pyridine hemochrome analysis. However, because of the presence of the cytochrome bc complex (Pereira *et al.*, 1999c), which dominates the EPR spectra and has a large contribution for the total amount of hemes B and C in the visible spectra, as well as the presence of hemes B from succinate dehydrogenase, it becomes difficult to determine a change in the expression of the cbb_3 terminal oxidase. A more clear result was obtained by HPLC analysis (see below) of heme extracts from cells harvested at the mid-exponential phase, when the oxygen level is still high, or at the late stationary phase, when the oxygen level is extremely low (virtually anaerobic conditions). A change in the relative proportion of

hemes B and A was observed, showing a decreased relative content of A-type hemes at the stationary phase (data not shown). Because of the amount of cells needed, all subsequent studies were performed with cells harvested at the late stationary phase.

Rhodothermus marinus membranes exhibit a respiratory rate of 10 nmolO₂/min mg of protein with TMPD as the electron donor at 40°C. Classical inhibitors of complex III had no inhibitory effect on the respiration rates (Pereira *et al.*, 1994).

The visible spectrum of the membrane extract (Fig. 1A) shows a Soret band with a maximum at 424 nm and α -bands corresponding to *c*- (at 552 nm) and *b* (at 558 nm)-type heme centers. Very low-intensity bands at ca. 444 and 605 nm, typical of heme-a centers are also observed. Heme analysis by pyridine hemochrome confirms the presence of A-, B-, and C-type hemes, in an approximate ratio of 1A :7B :14C

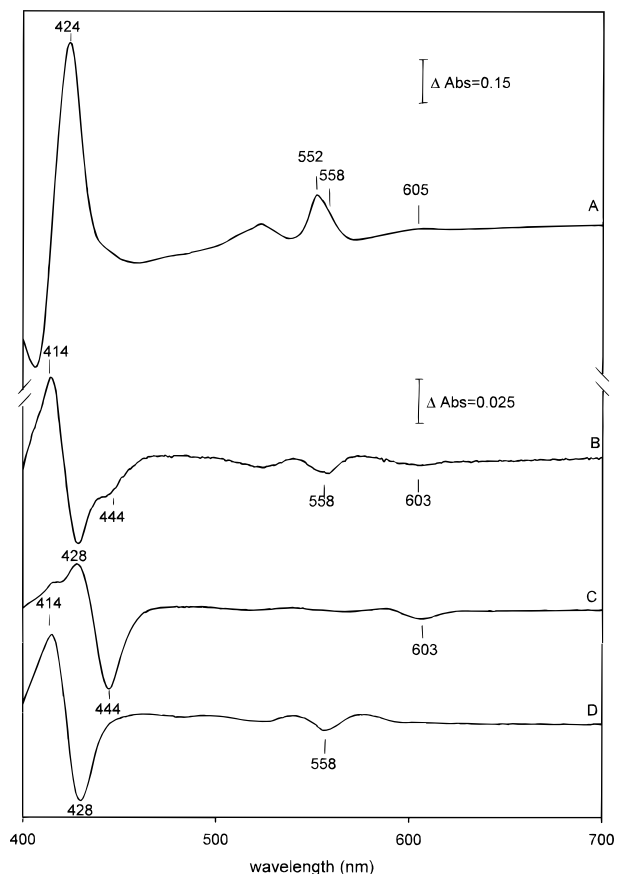


Fig. 1. (A) Dithionite-reduced minus oxidized visible spectrum of *R. marinus* membrane extract at room temperature. (B–D) Dithionite-reduced + CO minus dithionite-reduced visible spectra of *R. marinus* membrane extract (B), *caa*₃ oxidase (C), and *cbb*₃ oxidase (D) at room temperature.

analysis corroborated the presence of B- and A-type hemes (data not shown). There is no evidence for either O- or D-type hemes. Most interestingly, the A hemes are of the A_s type, which have a hydroxyethylgeranylgeranyl group instead of a farnesyl in its side chain (Lübber and Morand, 1994) (data not shown). These hemes are associated with the *caa*₃ oxidase (Pereira *et al.*, 1999b).

Reaction with carbon monoxide in the reduced state yields a drastic spectral resolution: the CO-difference spectrum obtained for *R. marinus* membrane extract (Fig. 1B) is characteristic of CO-bound cytochromes *a* and *b*. A ratio of 2.5 high-spin heme B per high-spin heme A is obtained.

The EPR spectra of *R. marinus* membranes show resonances centered at $g \sim 6$, due to high-spin hemes, and resonances characteristic of low-spin ferric hemes, with g_{\max} ranging from ~ 3.30 to ~ 2.78 , which accounts for at least five distinct species (Fig. 2A). The spectrum results from the contribution of the main heme complexes, namely, the *caa*₃ (Pereira *et al.*, 1999b) (Fig. 2B) and the *cbb*₃ oxidases (Fig. 2C and see below), at $g = 3.30$ and 2.93 , and the cytochrome *bc* complex, at $g = 3.32$, 3.02 , 2.80 , and 2.78 (Fig. 2D) (Pereira *et al.*, 1999c). In the $g \sim 2$ region, intense resonances due to the HiPIP and succinate dehydrogenase center S3 are observed (Pereira *et al.*, 1994, 1999a). Upon anaerobic addition of NADH (3 mM) or

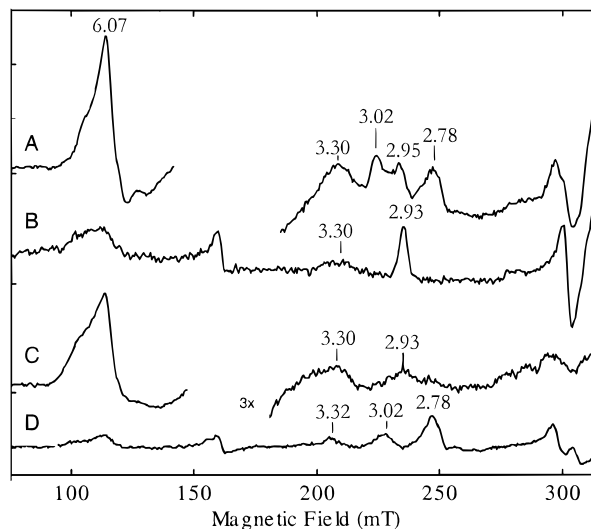


Fig. 2. EPR spectra of *R. marinus* oxidized membranes (A), *caa*₃ oxidase (B), *cbb*₃ oxidase (C), and of cytochrome *bc* complex (D) at 10 K. Microwave frequency, 9.64 GHz; microwave power, 2.4 mW; modulation amplitude, 0.9 mT. A signal at $g \sim 4.3$ was removed for clarity.

menadiol (1 mM) to the membrane preparation, all heme resonances vanish. A new well-defined resonance develops with $g_{\max, \text{med}} = 2.88, 2.30$, which is associated with the cytochrome *bc* complex and disappears with longer incubation with either reductant (Pereira *et al.*, 1999c), in agreement with the redox titration data. As already observed (Pereira *et al.*, 1994, 1999a), resonances characteristic of a Rieske center were not detected, which suggests the absence of a typical *bc*₁ complex and corroborates the absence of any effect upon addition of typical inhibitors of this complex. In the soluble fraction only, a ferredoxin (our own unpublished data) was detected as a soluble redox carrier; neither cytochromes nor soluble Rieske proteins, as in *Sulfolobus sp.* Strain 7 (Iwasaki *et al.*, 1995), could be observed.

An overview of the redox behavior of all heme components present in *R. marinus* membranes was obtained by redox titrations monitored by visible spectroscopy (Fig. 3), which allowed for the establishment of a range of redox potentials of all heme centers. Because of extensive spectral and redox overlap of the several heme centers, a complete deconvolution was not attempted. The data was analyzed by following the changes in absorbance at the major Soret band (424 nm) and the α -bands at 552 and 558 nm. The range of reduction potentials of the heme centers could be clearly defined, having as upper and lower limits $\sim +250$ and -60 mV, respectively. Four major transitions were observed, with reduction potentials of approximately 250, 110, 80, and -60 mV (Fig. 3C). While the titration curve obtained with the data at 552 nm (main contribution from *c*-type hemes) follows mono-electronic Nernst curves, at 558 nm, where there is a larger contribution of the *b*-hemes, there is a clear deviation from $n = 1$, and a good fit is obtained with $n = 2$. The same behavior was observed with the cytochrome *bc*, which may indicate positive cooperativity between the redox centers involved in this last transition. It is worth stressing that the last optical species presents a shoulder at ~ 419 nm, because of the cytochrome *bc* complex (Pereira *et al.*, 1999c) [Fig. 3 B(D–C)]. Within experimental error, the same level of complete reduction is obtained using dithionite, NADH, succinate, or menadiol as reductants. Representative redox spectra of the different transitions are presented in Fig. 3A,B. A detailed analysis and the assignment of each of these transitions was obtained by titrating each individual complex (following section and Pereira *et al.*, 1999bc).

cbb₃ Oxidase

Isolation and Identification of Oxidase Gene

The sequence of the PCR product was compared with the sequence databases (Fig. 4). As expected, the product shows a very strong identity with FixN-type terminal oxidases. This result and the sequencing of the gene cluster coding for a COX-type oxidase (our unpublished data) indicates that *R. marinus* genome contains at least two distinct genes coding for two different types of terminal oxidases of the heme–copper superfamily. In fact, a *caa₃* (Pereira *et al.*, 1999b) and a *cbb₃* oxidases were isolated from *R. marinus* (see next sections).

Biochemical and Spectroscopic Characterization

A *cbb₃* oxidase was partially purified. As mentioned in the Section on Materials and Methods, further purification steps did not change any spectral feature or the electrophoretic pattern. The protein used for further studies showed in tricine SDS-PAGE, five bands with apparent molecular masses of 64, 57, 36, 26, and 13 kDa (data not shown). Only the band with 26 kDa was detected by heme staining. As reported for other preparations of *cbb₃*-type oxidases, several subunits are found (Gray *et al.*, 1994; Garcia-Horsman *et al.*, 1994; de Gier *et al.*, 1996; Keefe and Maier, 1993; Tamegai and Fukumori, 1994); the major difference is the presence of only one heme-stained subunit. The other C-type heme binding subunit may have been lost during purification, as reported for *Paracoccus denitrificans* (de Gier *et al.*, 1996), or be absent in *R. marinus*. All the spectroscopic data (see below) are consistent with a lower cytochrome *c* content in the oxidase from this bacterium.

The reduced minus oxidized spectrum of this oxidase presents an asymmetric α -band at 553 nm with a shoulder at 558 nm and a Soret band at 425 nm, indicating the presence of hemes of the *b* and *c* types (Fig. 5; Table I). A better resolution of this spectrum is obtained at liquid nitrogen temperature, in which in the α -band region two peaks at 549 (heme *c*) and 555 (heme *b*) are clearly observed (Fig. 5, insert). In the absolute spectrum of the oxidized enzyme, a broad band at ca. 630 nm, typical of high-spin protoheme centers, is observed and no band at 695 nm was detected, indicating the absence of a methionine ligand to any of the heme centers of this complex (data not

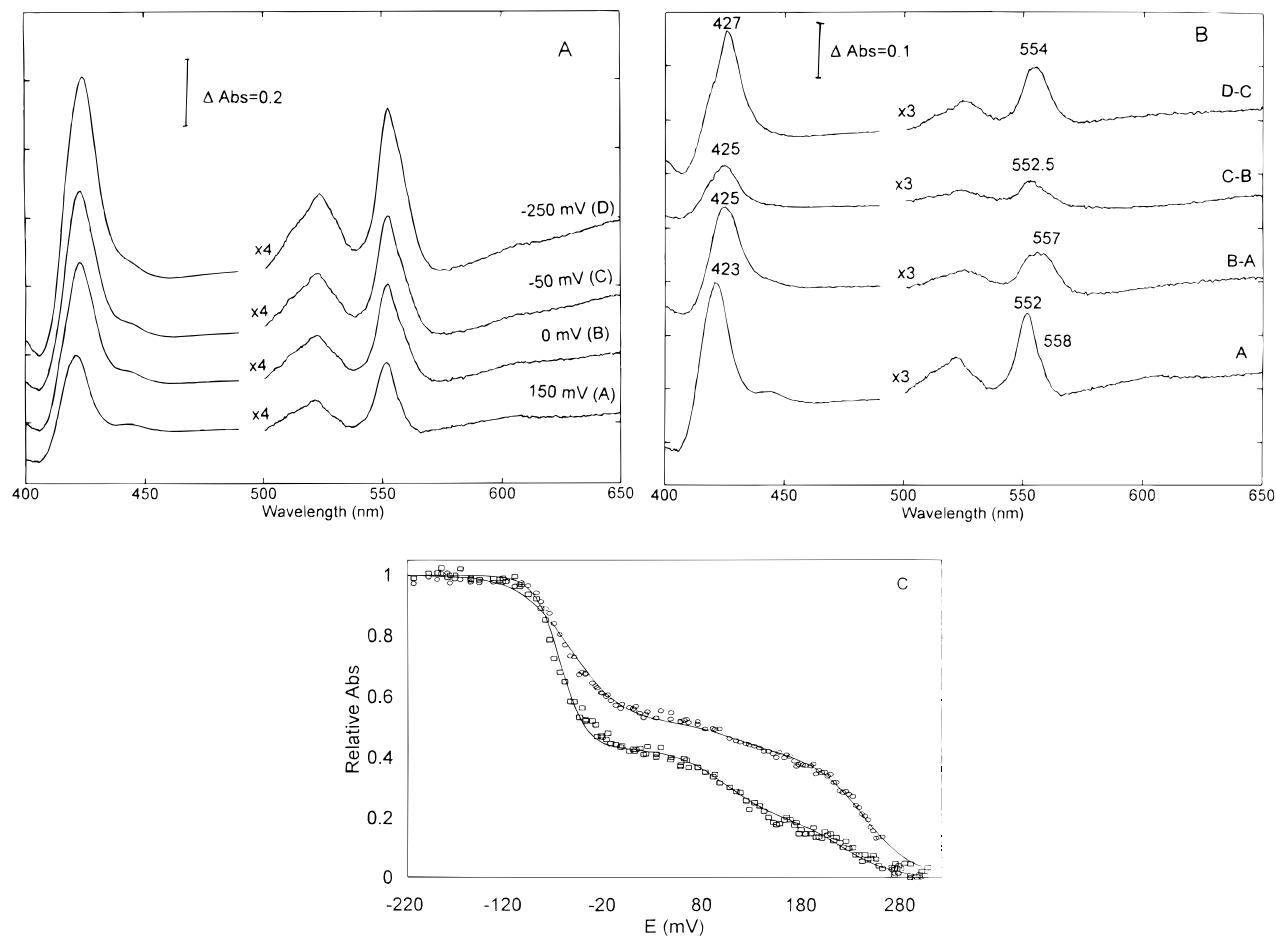


Fig. 3. Visible redox titration of *R. marinus* membrane extract. (A) Redox spectra at selected redox potentials. (B) Difference spectra at each transition. (C) Change in absorbance at 552 nm (circles) and 558 nm (squares). The solid lines are the best fit obtained using three Nernst equations with $n = 1$ and $E_0 = 250$ mV (42%), 110 mV (10%) and -55 mV (48%) for 552 nm and $E_0 = 220$ mV (20%), 110 mV (20%), and -60 mV (60%) for 558 nm.

shown). A stoichiometry of 1 heme C per 1 heme B was determined by pyridine hemochrome. The CO difference spectrum (Fig. 1D; Table I) is identical to the characteristic CO spectrum of high-spin ferrous B heme centers (Wood, 1984). The CO spectra of the *cbb*₃- and *caa*₃- type oxidases (Pereira *et al.*, 1999b) fill all the features present in the CO spectrum of the membrane extract, suggesting that these are, in fact, the only two oxidases expressed (Fig. 1).

The EPR spectrum of the partially purified oxidase shows the presence of a high-spin heme center at $g \sim 6.07$ and low-spin ferric heme centers with g_{\max} values around 3.30 and 2.93 (Fig. 2C). The resonances are very broad in all preparations studied and the addition of glassing agents, such as ethylene glycol, did not improve the resolution. The oxidase copurifies with a small amount of the HiPIP protein, which was always

found to be a contaminant of the several preparations studied (data not shown). A Cu_A-type signal in the $g \sim 2$ region was not observed in any preparation.

The redox titration of the *cbb*₃ complex was deconvoluted into three different transitions (Fig. 6), each described by single Nernst equations with reduction potentials of 195, 120, and -50 mV. Although the actual “shape” of the experimental data seem to indicate possible positive and negative redox cooperativity (evidenced by the deviation from $n = 1$ Nernst equations), at present it was not attempted to fit the data with interactions since an unambiguous solution would not be obtained. The first and second transitions are due to the reduction of a heme *c* and a heme *b*, respectively (Table I). The third transition shows a spectrum having a broad α -band at 556 nm and a Soret band at 427 nm. The relative intensities of each of

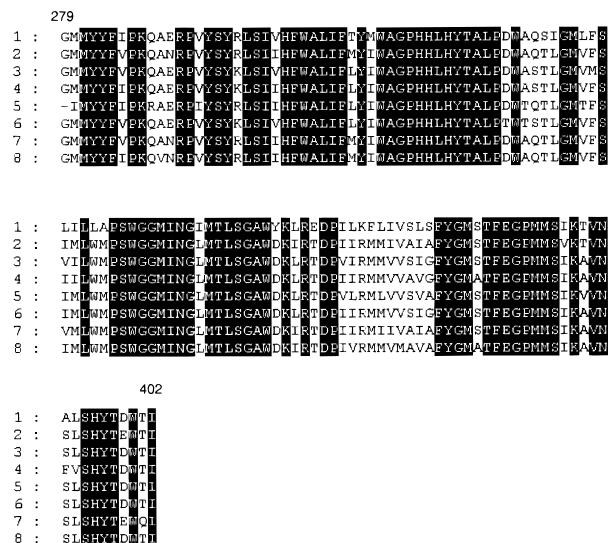


Fig. 4. Alignment of *R. marinus* PCR product with highest homologous sequences obtained by comparison with protein database using the NCBI Entrez protein sequence search. *FixN* product, (1) *R. marinus*, (2–8) *cbb₃* type oxidases from (2) *Rhizobium leguminosarum* (acc. no. AAB58264), (3) *Rhodobacter capsulatus* (acc. no. AAC46108); (4) *Paracoccus denitrificans* (acc. no. AAC44516); (5) *Bradyrhizobium japonicum* (acc. no. Q03073); (6) *Rhodobacter sphaeroides* (acc. no. AAB02556); (7) *Rhizobium etli* (acc. no. AAC15888); (8) *Agrobacterium tumefaciens* (acc. no. P98055); sequence numbering is referred to 2. Totally conserved residues are shaded in black.

these three optical species, measured both by relative absorbance (at the Soret band) and area (at the α -band), is 1:1:2, in agreement with the relative heme content determined to be 1 heme B per 1 heme C. The last optical species was assigned by performing spectra using ascorbate (which reduces the first two cytochromes) and dithionite as reductants and reacting the enzyme with CO in the presence of each reductant. The bleaching of the band at 630 nm and reaction with CO was observed only upon dithionite reduction, indicating that the high-spin heme *b* contributes to the last optical species. In fact, ferrous high-spin B-type hemes usually show a single broad band at 555–560 nm (Wood, 1984). Because of the relative intensity of this last transition, its absorption characteristics (including a clearly resolved β band at 525 nm) and the heme stoichiometry determined, a heme *c* must also contribute to this optical species having within experimental error a reduction potential close to that of heme *b₃*. Reduction potentials associated with each heme center of this complex were observed in the titration of the membrane extract.

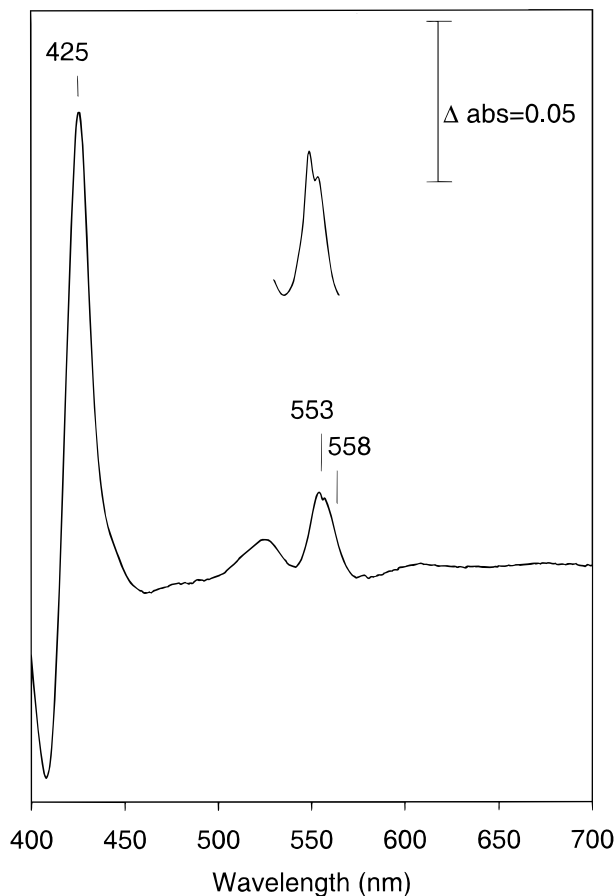


Fig. 5. Dithionite-reduced minus -oxidized visible spectra of *R. marinus cbb₃* oxidase at room and at liquid nitrogen (insert) temperatures.

This complex oxidizes TMPD with turnover numbers of 209 min⁻¹ (mole TMPD/mole heme B/min), at 65°C. Since it has oxygen reductase activity, contains C- and B- type hemes, and one of the hemes is high-spin and binds CO, it is referred to as a *cbb₃* oxidase.

Table I. Maxima of Redox Visible Spectra and Troughs for CO Difference Spectra for Each Cytochrome Component and Respective Reduction Potentials for *R. marinus cbb₃* Terminal Oxidase at pH 7

Soret (nm) (cyt. type)	α (nm) (cyt. type)	CO spectra, nm troughs (peak)	E' (mV)
420 (<i>c</i>)	552 (<i>c</i>)		195
427 (<i>b</i>)	558 (<i>b</i>)		120
427 (<i>c</i> + <i>b₃</i>)	556 (<i>c</i> + <i>b₃</i>)	428 (414), 558	-50

^a Shoulder.

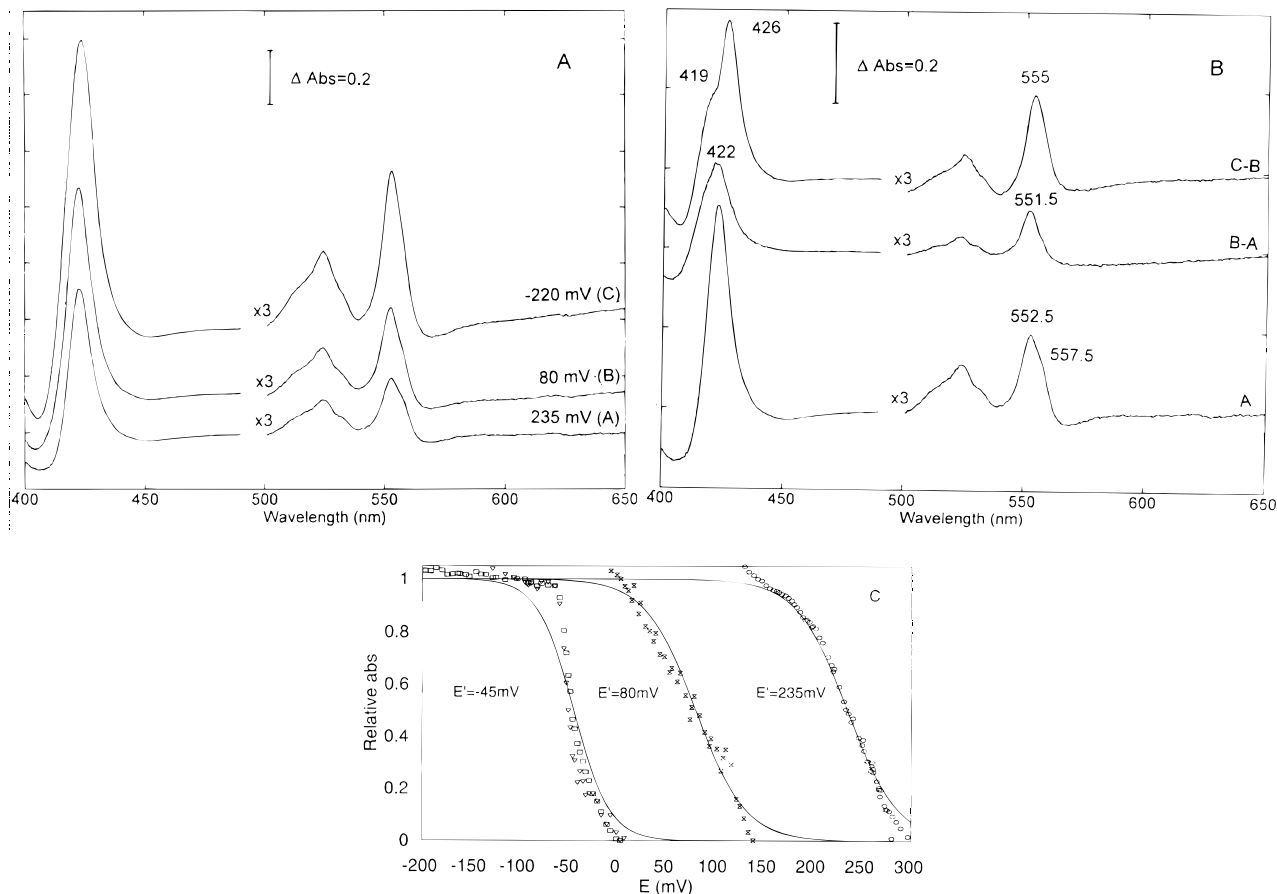


Fig. 6. Visible redox titration of *R. marinus cbb₃* oxidase. (A) Redox spectra at selected redox potentials. (B) Difference spectra at each transition. (C) Data obtained at the Soret band maxima; solid lines were obtained using Nernst equations with the potentials presented in Table I.

This assignment is strongly supported by the observation of a *FixN*-type gene in *R. marinus* genome (Fig. 4). The observation of only one subunit containing C-type heme(s), together with the visible spectroscopic and redox data, suggests that this subunit contains two C-type hemes and that a monohemic subunit, reported for other *cbb₃* oxidases, is not present in the preparations of *R. marinus* oxidase. The low activity observed is most probably due to TMPD being a poor electron donor to this oxidase, which may, in part, result from the low reduction potentials of the oxidase in relation to TMPD (+260 mV, Dawson *et al.*, 1986). The integrity of the enzyme preparations is assured by the identity of the spectral and redox properties of the purified enzyme with those observed for the full membrane extract. The physiological electron donor to this oxidase remains to be found. *Rhodothermus marinus* HiPIP, under the conditions tested, appears to be also a poor electron donor (Pereira *et al.*, 1999c), which

may be a consequence of the possible lack of the extra heme containing subunit.

DISCUSSION

The respiratory chain of *R. marinus* presents some unique properties (Table II), mainly concerning its complex III, which is a novel multihemic cytochrome *bc* and its major electron carrier between this complex and a *caa₃* terminal oxidase, which is a high-potential iron-sulfur protein (HiPIP) (Pereira *et al.*, 1994, 1999a,b,c). Its characterization was further extended by the identification of a *cbb₃* oxidase. Thus, like most bacteria, *R. marinus* presents a branched respiratory chain, at the level of its terminal oxidases. These oxidases, together with the cytochrome *bc* complex and a small membrane-bound cytochrome *c* and succinate dehydrogenase (our unpublished data), contain most

Table II. Reduction Potentials for Each Cytochrome Component of *R. marinus* Respiratory Complexes at pH 7

Activity	Cytochrome	E' ₀ , mV (heme center)
Oxygen reductase, HiPIP oxidase ^a ? oxidase ^b	<i>caa</i> ₃ <i>cbb</i> ₃	260 (C), 255 (A), 180 (A ₃) 195 (C), 120 (B), -50 (C + B ₃)
Menaquinol:HiPIP oxidoreductase ^c	<i>bc</i>	235 (B), 235 (C), 80 (C), -45 (C + C)
Succinate: menaquinone oxidoreductase ^d	<i>b</i>	75 (B), -65 (B)
Electron carrier ^d	<i>c</i>	267 (C)

^a Pereira *et al.* 1999b.^b This work.^c Pereira *et al.*, 1999c.^d Our unpublished data.

heme centers present in *R. marinus* membranes, as determined by the visible, CO difference, and EPR spectra, as well as by redox titration data. In contrast with typical aerobic respiratory chains, *R. marinus* heme centers have relatively low reduction potentials; in particular, the higher potential is $\sim +260$ mV, much lower than those associated with at least the terminal oxygen reductases (generally close to $+350$ mV). The range of reduction potentials obtained for the membrane extract fully agrees with those determined for the different heme centers of the isolated respiratory complexes (Table II). The *R. marinus cbb*₃ oxidase is the first example of this type of oxidase in an organism outside the proteobacteria group, as well as in a thermophile.

The expression of two oxidases, both containing extra redox centers when compared to the mitochondrial enzyme may be a consequence of the need for more efficient oxygen reduction complexes, in the environmental conditions where *R. marinus* thrives: high temperatures and low dioxygen availability. In *R. marinus*, the two oxidases are always expressed under the tested conditions, although the data points to a higher level of expression of the *caa*₃ oxidase when the oxygen content of the medium is higher. This suggests that the *cbb*₃ oxidase has a higher level of expression under lower oxygen availability, as generally observed for this type of oxidase (*e.g.*, Keefe and Maier, 1993; Preisig *et al.*, 1996). According to the work of Verkhovskiy and co-workers (Verkhovskiy *et al.*, 1999), four electrons are not sufficient for total proton translocation, which is only observed upon re-reduction of the enzyme with at least one electron. Oxidases with extra redox centers may provide these extra electrons, enhancing its proton translocation capability.

ACKNOWLEDGMENTS

We would like to thank Dr. Jose Castresana for providing the primers used for PCR, Marko Hyvönen for all the help in the molecular biology experiments, and the IBET fermentation plant for the bacterial growth. *Rhodothermus marinus* strains were a kind gift from Prof. M. da Costa. Manuela Pereira is recipient of a grant from PRAXIS XXI program (BD/2758/94). The work was supported by PRAXIS XXI grants and by European Union G-Project on Biotechnology of Extremophiles (Bio4-CT96-0488).

REFERENCES

- Alfredsson, G. A., Kristjansson, J. K., Hjörleifsdóttir, S., and Stetter, K. (1988). *J. Gen. Microbiol.* **134**, 299–306.
- Andrésson, O. S., and Fridjónsson, O. H. (1994). *J. Bacteriol.* **176**, 6165–6169.
- Anemüller, S., Schmidt, C. L., Pacheco, I., Schäfer, G., and Teixeira, M. (1994). *FEMS Microbiol. Lett.* **117**, 275–280.
- Ausubel, F. M., Brent, R., Kingston, R. E., Morre, D. D., Smith, J. A., Seidman, J. C., and Struhl, K. (1995). *Current Protocols in Molecular Biology*, Wiley, New York.
- Bell, L. C., Richardson, D. J., and Ferguson, S. J. (1992). *J. Gen. Microbiol.* **138**, 437–443.
- Berry, E. A., and Trumpower, B. L. (1987). *Anal. Biochem.* **161**, 1–15.
- Bonora, P., Principi, I., Monti, B., Ciurli, S., Zannoni, D., and Hochkoeppler, A. (1999). *Biochim. Biophys. Acta* **1410**, 51–60.
- Dawson, R. M. C., Elliott, D. C., Elliott, W. H., and Jones, K. M. (1986). *Data for Biochemical Research*, 3rd edn., Oxford University Press, Oxford.
- de Gier, J.-W., Schepper, M., Reijnders, W. N. M., van Dyck, S. J., Slaatboom, D. J., Warne, A., Saraste, M., Krab, K., Finel, M., Stouthamer, A. H., van Spanning, R. J. M., and van der Oost, J. (1996). *Mol. Microbiol.* **26**, 1247–1260.
- Garcia-Horsman, J. A., Berry, E., Shapleigh, J. P., Alben, J. O., and Gennis, R. B. (1994). *Biochemistry* **33**, 3113–3119.
- Goodhew, C. F., Brown, K. R., and Pettigrew, G. W. (1986). *Biochim. Biophys. Acta* **852**, 288–294.

- Gray, K., Grooms, M., Myllykallio, H., Moomaw, C., Slaughter, C., and Daldal, F. (1994). *Biochemistry* **33**, 3120–3127.
- Hochoeppler, A., Kofod, P., and Zannoni, D. (1995). *FEBS Lett.* **375**, 197–200.
- Iwasaki, T., Isogai, Y., Iizuka, T., and Oshima, T. (1995). *J. Bacteriol.* **177**, 2576–2582.
- Keefe, R., and Maier, R. (1993). *Biochim. Biophys. Acta* **1183**, 91–104.
- Kristjansson, J. K., and Stetter, K. O. (1992). In *Thermophilic Bacteria* (Kristjansson, J. K., ed.), CRC Press, Boca Raton, Florida, pp. 1–18.
- Lübber, M., and Morand, K. (1994). *J. Biol. Chem.* **269**, 21473–21479.
- Madigan, M. T., Martinko, J. M., and Parker, J. (1997). *Biology of Microorganisms*, 8th edn, Prentice-Hall, New Jersey.
- Moreira, L., Nobre, M. N., Sá-Correia, I., and da Costa, M. S. (1995). *System. Appl. Microbiol.* **19**, 83–90.
- Nunes, O. C., Donato, M. M., and da Costa, M. S. (1992). *System. Appl. Microbiol.* **15**, 92–97.
- Pereira, M. M., Antunes, A. M., Nunes, O. C., Costa, M. S., and Teixeira, M. (1994). *FEBS Lett.* **352**, 327–330.
- Pereira, M. M., Carita, J. N., and Teixeira, M. (1999a). *Biochemistry* **38**, 1276–1283.
- Pereira, M. M., Santana, M., Mendes, J., Soares, C. M., Carita, J. N., Fernandes, A. S., Saraste, M., Carrondo, M., and Teixeira, M. (1999b). *Biochim Biophys Acta* **1413**, 1–13.
- Pereira, M. M., Carita, J. N., and Teixeira, M. (1999c). *Biochemistry* **38**, 1268–1275.
- Preisig, O., Zufferey, R., Thöny-Meyer, L., Appleby, C. A., and Hennecke, H. (1996). *J. Bacteriol.* **178**, 1532–1538.
- Richardson, D. J., McEwan, A. G., Jackson, J. B., and Ferguson, S. J. (1989). *Eur. J. Biochem.* **185**, 659–669.
- Schägger, H., and von Jagow, G. (1987). *Anal. Biochem.* **166**, 368–379.
- Tamegai, H., and Fukumori, Y. (1994). *FEBS Lett.* **347**, 22–26.
- Thompson, J. D., Gibson, T. J., Plewniak, F., Jeanmougin, F., Higgins, D. G. (1997). *Nucleic Acid Res.* **25**, 4876–4882.
- Verkhovskiy, M. I., Jasaitis, A., Verkhovskaya, M. L., Morgan, J. E., and Wikstrom, M. (1999). *Nature* **400**, 480–483.
- Watters, C. (1978). *Anal. Biochem.* **88**, 695–698.
- Wood, P. M. (1984). *Biochem. Biophys. Acta* **768**, 293–317.